



Warr, P. A., & Hilton, G. S. (2010). Configurable microwave structures for software defined (and cognitive) radio front ends. In 2010 Mediterranean Microwave Symposium (MMS), Guzelyurt. (pp. 91 - 97). Institute of Electrical and Electronics Engineers (IEEE). 10.1109/MMW.2010.5605142

Link to published version (if available):  
[10.1109/MMW.2010.5605142](https://doi.org/10.1109/MMW.2010.5605142)

[Link to publication record in Explore Bristol Research](#)  
PDF-document

## University of Bristol - Explore Bristol Research

### General rights

This document is made available in accordance with publisher policies. Please cite only the published version using the reference above. Full terms of use are available:  
<http://www.bristol.ac.uk/pure/about/ebr-terms.html>

### Take down policy

Explore Bristol Research is a digital archive and the intention is that deposited content should not be removed. However, if you believe that this version of the work breaches copyright law please contact [open-access@bristol.ac.uk](mailto:open-access@bristol.ac.uk) and include the following information in your message:

- Your contact details
- Bibliographic details for the item, including a URL
- An outline of the nature of the complaint

On receipt of your message the Open Access Team will immediately investigate your claim, make an initial judgement of the validity of the claim and, where appropriate, withdraw the item in question from public view.

# Configurable Microwave Structures for Software Defined (and Cognitive) Radio Front Ends

Dr Paul Warr, Dr Geoff Hilton  
Department of Electrical and Electronic Engineering  
University of Bristol  
Bristol, UK

**Abstract**— Both Software Defined Radio and Cognitive Radio require a flexible transceiver front end. This paper introduces solutions to two important features of such a device; the antenna and the filter. These are both microwave resonant structures and so share design trade-offs and restrictions; in this application they must both offer some degree of tunability or wideband performance. MEMS technology is proposed as the enabler for reconfigurability in the distributed microwave structures. This technology overcomes the shortcomings of both large-scale mechanical devices and semiconductor-based solutions.

**Keywords**- *frequency-tuning, bandwidth-tuning, filters, antennas, software-defined radio, cognitive radio*

## I. INTRODUCTION

### A. Flexible Radio

The term Software Defined Radio (SDR) refers to a transceiver which supports variations in operating frequency, bandwidth and modulation scheme; all of which are defined entirely by software. The transceiver will, therefore, be capable of operating on any current or future standard by a change in status [1].

The term Cognitive Radio (CR) refers to an extension of SDR to a system that is aware of its user's needs, available resources and operational limitations [2]. The ideal system would not only be adaptable to any standard, but also be capable of supporting itself and other devices in the most efficient way. Practical issues, such as power levels, radiation pattern control and data management, would all be continuously optimized for the current scenario [3].

The literature on advanced radio systems depicts many possible operation scenarios, such as the avoidance of strong interference at a specific band, applying a tunable notch at a disruptive blocker [4], or moving into some under-utilized spectrum [5], and others which rely heavily on the efficient use of tunable microwave filters and antennas. At the device-level, tuning is usually accompanied by degraded performance as it presents a trade-off between the tuning range and degradation in insertion-loss. This is due to the matching-process being frequency dependent which complicates the feeding strategy as it too needs to become flexible.

### B. Front End Requirements

The extent to which a flexible transceiver can be implemented will inevitably depend on the hardware performance. Positioning A/Ds and D/As at the antenna terminals is not currently possible at commercial wireless systems operating frequencies (Table 1). Current transceiver designs typically use a superheterodyne [6] or direct conversion architecture [7]; these involve mixing down the received signals to lower frequencies in order to circumvent the limitations of A/D conversion and digital processing speed. Flexibility in operational frequency requires either tunability or wideband operation of the system's filters, amplifiers, local oscillators and other components. Within restrictions, some transceiver designs have been able to achieve this [8]; though full operation is only currently possible with the lower frequency standards, such as in some military applications.

TABLE I. NON EXHAUSTIVE SUMMARY OF COMMERCIAL COMMUNICATIONS FREQUENCIES

Standard	Range(MHz)	Standard	Range(MHz)
GSM850	824-984	IEEE802.11a	515-5925
GSM900	890-960	IEEE802.11b	2400-2497
E-GSM	880-925	IEEE802.11g	2400-2484
R-GSM	876-960	IEEE802.15.3a(UWB)	3100-5150
GSM1800	1710-1880		5825-10600
GSM1900	1850-1990		3600-6900
PCS (USA)	1910-1990		7450-10200
IS-136	1850-1990	IEEE802.16a	2000-11000
WCDMA 3GPP/FDD	1710-2110	IEEE802.16	10000-66000
WCDMA 3GPP/TDD	1850-2025	IEEE802.20	circa 3500
Bluetooth	2402-2480		

Over the many communication standards identified in TABLE I a wide variety of digital modulation schemes are employed. From the perspective of the RF front end, the details of these are of little interest. The functionality of the front end may be defined only in terms of the channel bandwidths, centre frequencies, noise figure, linearity requirements and power limits.

### C. Making Distributed Resonant Structures Configurable

Establishing the appropriate features of the tunable distributed structure is the principal design challenge. The form factor of the tuning elements themselves may be accommodated by

variations in the chosen substrate dielectric constant and thickness. MEMS (Micro Electro-Mechanical Structures) offer an appropriate platform for the tuning elements due to their excellent linearity, isolation, low on-loss and power handling characteristics.

Significant theoretical and experimental work is required in order to establish an appropriate design methodology to make a distributed structure tunable. For this, the use of (currently expensive) MEMS devices is not required.

In this paper two structures are presented, one each for the antenna and filter.

- For the filter, a lumped-distributed coupled line filter is proposed with centre frequency and bandwidth tuning via inter resonator coupling and resonator length control.
- For the antenna, a dual-fed cavity-backed linear slot antenna is proposed with frequency tuning via both slot length control and input susceptance control.

## II. TUNABLE FILTER STRUCTURE

### A. Resonator topology

Here, a lumped-distributed, coupled transmission-line resonator approach is proposed as a solution for the flexible filter requirement. This structure is suitable for MEMS contact and capacitive switches as controlling elements. The limit of configurability comes from the electrical size of transmission-lines and the placement density of the RFMEMS devices.

A combline topology is adopted, comprising pairs of grounded, quarter-wavelength, coupled resonators (Fig. 1). The advantages of this topology are three-fold; firstly, only a single grounding switch is in-circuit regardless of the selected length, therefore the impact of resistive switch losses on resonator Q remains constant. Secondly, it retains a constant overlap region and coupling factor regardless of the coupled line length. Finally, because the electro-magnetic (EM) coupling between the transmission-lines is in anti-phase to the lumped capacitive coupling, very low coupling coefficients can be obtained regardless of coupled-line spacing.

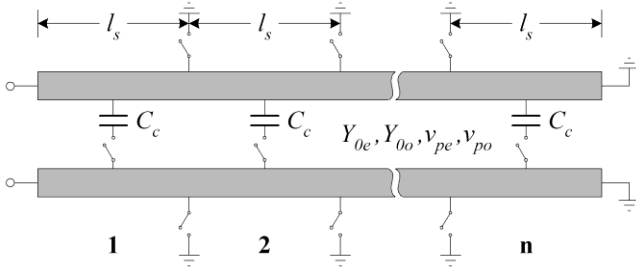


Figure 1. Lumped-distributed, quarter-wave, coupled resonators.

### B. Inter-resonator coupling

Using the formulation developed in [9] the coupling coefficient of the lumped-distributed coupled-line structure can be found from its simulated frequency response. Typical results are shown in Fig. 2 where the coupling coefficient for a pair of coupled microstrip lines is plotted against the total lumped capacitance for various values of coupled line spacing,

s. The change in gradient of the coupling coefficient, from negative to positive, is indicative that, for this coupled-line configuration, the distributed electro-magnetic coupling is primarily magnetic in nature and is in anti-phase to the direct capacitive coupling. The result is that, at low values of lumped coupling capacitance, the coupling coefficient is actually reduced allowing the coupling coefficient, and therefore the filter bandwidth, to be controlled down to a very low value without the need for large coupled-line spacing.

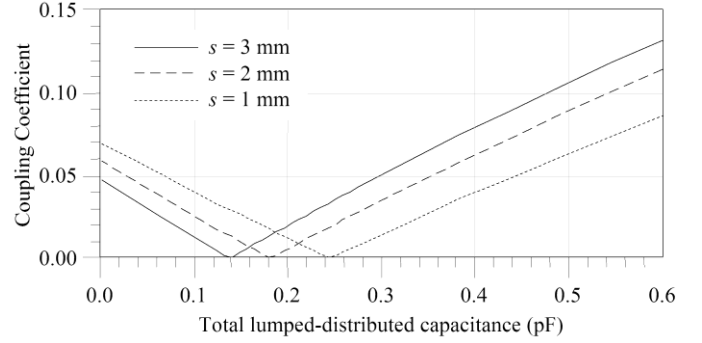


Figure 2. Coupling coefficient of lumped-distributed coupled lines indicating that the capacitive coupling is in anti-phase to the EM coupling.

### C. Filter Topology

A modified combline filter topology was synthesized and realized [10]. The filter is constructed by connecting the near-side resonators of adjacent sections to form a series of half-wavelength resonators coupled to each other along half their length. The filter differs from a quarter-wave combline topology in this respect but the difference is necessary in order to accommodate the grounded MEMS switches. Unfortunately, the resulting structure supports passbands at all harmonic frequencies. This can be observed in Fig. 4, where the responses of an ideal 5th order lumped-distributed coupled resonator filter is plotted alongside that of the prototype filter.

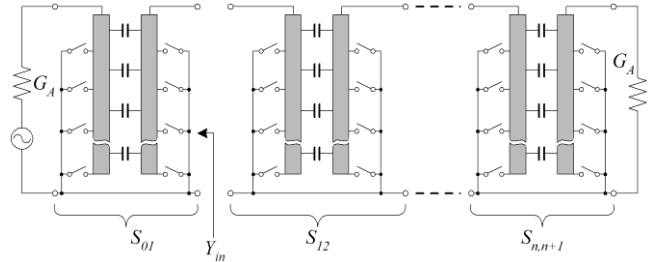


Figure 3. Lumped-distributed coupled-resonator filter

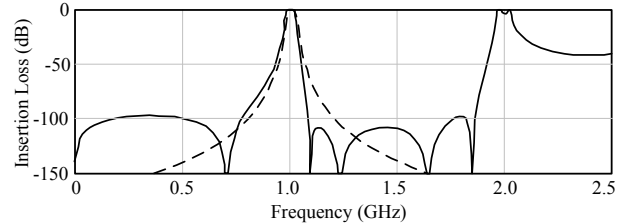


Figure 4. Response of an ideal 5th order synthesised lumped-distributed coupled-resonator filter (solid line) compared to the prototype filter response (broken line).

Once initial design values have been selected and the filter realized it is tuned by the discrete switching of ground connections and coupling capacitors. Since the tuning is not continuous only certain values of centre frequency and bandwidth can be obtained. Furthermore, the relationships between coupling capacitance, resonator length, fractional bandwidth and centre frequency are not linear.

The coupling capacitance acts to reactively load the transmission lines, altering their odd-mode characteristic impedance and phase velocity. As the coupling capacitance is tuned, the effective phase velocity and consequently, the resonant frequency of the transmission lines is altered. To achieve the impedance transformation required in practical transmission-line filters the coupling capacitors of the filter end sections must be significantly larger than those of the interior sections. Changing the bandwidth involves scaling the inter-resonator coupling throughout the filter and the disproportionate size of the end section coupling capacitors means that their scaling has a greater effect on the phase velocity. This leads to a misalignment of end and interior section resonant frequencies, ultimately distorting the filter shape.

#### D. Filter Demonstrator Results

A third order filter with 16 tunable segments was designed and fabricated based on a Butterworth prototype (Fig.5). A coplanar waveguide medium was used as it allows well-defined and easily adjustable ground connections for the resonators. For prototyping purposes, the transmission-line lengths and lumped coupling capacitance were adjusted manually through the use of removable printed links to ground, and surface-mount 0603-size capacitors. The filter was designed to have a maximum fractional bandwidth of 15% with all coupling capacitors in circuit. The design centre frequency tuning range of the filter was from 350 MHz to 1.4 GHz.

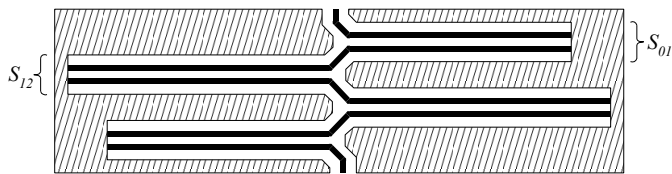


Figure 5. Diagram of experimental lumped-distributed coupled-line filter.

A selection of the 16 possible tuning states is shown in Fig. 6 along with the corresponding simulated responses. The filter gives almost constant fractional bandwidth across the complete tuning range except for a slight reduction at low values of coupled-line length (from 14% to 11.5%). The variation in insertion loss across the tuning range is also minimal. This reflects a constant unloaded Q of the resonators regardless of tuning position.

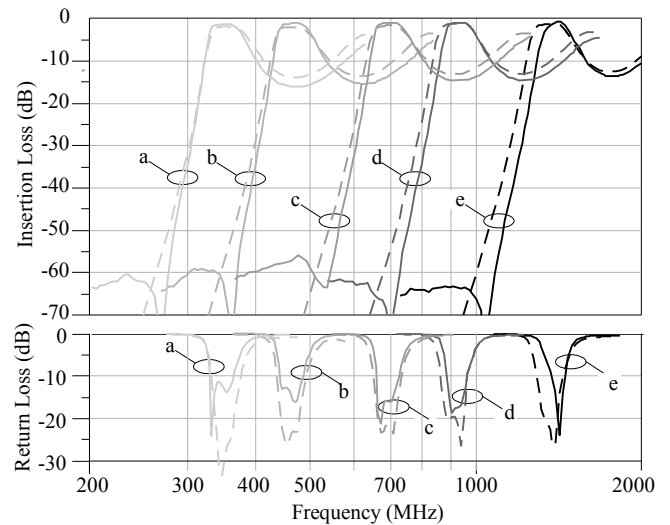


Figure 6. Simulated (broken line) and measured (solid line) results for five of the 16 possible tuning states of the experimental lumped-distributed coupled-line filter.

The bandwidth tuning capability of the filter is demonstrated in the practical results of Fig. 7: a centre frequency of 540MHz is maintained with ten example bandwidths. It is important to note that this is a discrete implementation and, therefore, continuous tuning of either bandwidth or frequency is not possible. As there is interrelationship between the two when the state of a given tuning element is changed, the response is non linear. Within the tuning space bounded by the extremes of bandwidth and centre frequency there are regions where a good filter shape factor is maintained and also regions where the shape factor is degraded.

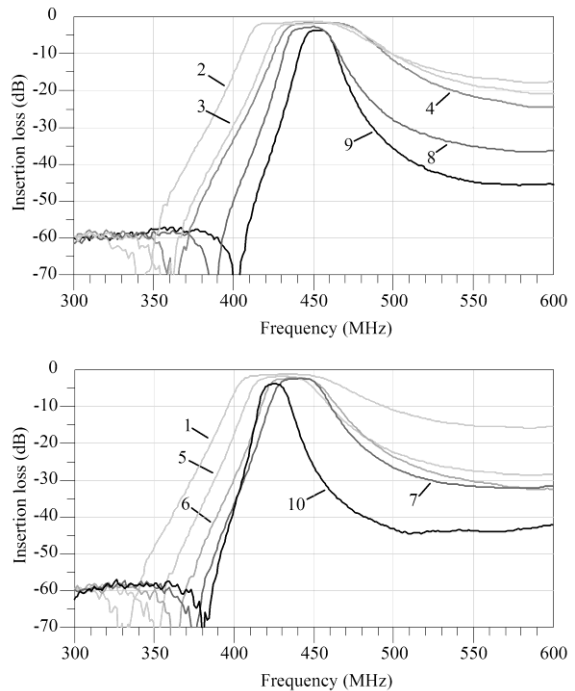


Figure 7. Measured insertion loss of experimental lumped-distributed coupled-line filter for 10 bandwidth tuning points (separated in to two plots for clarity).

An essential aspect of tunable filter design is the effect of the tuning mechanism on the filter insertion loss. Simulations using realistic values for the contact resistance ( $0.5\Omega$ ) and  $Q$  (50) of the RFMEMS contact and capacitive switches show that the unloaded  $Q$  of the resonators varies from a nominal value of 28 by only 21%, across both frequency and bandwidth tuning ranges. This indicates that the filter structure is relatively independent of the number of tuning elements employed.

### III. TUNABLE ANTENNA STRUCTURE

#### A. Antenna-specific Requirements

Antennas are most efficient when operated at the resonant frequencies of the structure, and the bandwidth capability is generally a function of the volume (or ‘openness’) of the structure. For instance, horn antennas or bow-tie dipoles have wider bandwidths than microstrip patch antennas, where the substrate thickness (generally less than a twentieth of a wavelength) significantly reduces the bandwidth down to a few percent [11]. Lossy substrates may give the appearance of wider bandwidth, but this inefficiency is translated into less (radiated) power. The problem, therefore, is that in order to achieve the operating bandwidth required for a flexible transceiver covering commercial wireless standards, the structures should not be ‘confined’ as is often the case when trying to accommodate the antenna in a small portable terminal.

A further issue is that operating an antenna over a wide bandwidth may excite different modes in the structure leading to considerable changes in radiation pattern performance (signal levels and polarization) – nulls may form in the pattern in the required signal direction. In the commercial mobile radio terminal environment, for reasons of manufacturability and very low cost, printed antennas are favored with antennas such as Planar Inverted F Antennas (PIFA) fabricated on cheap substrates dominating the fixed-frequency solutions.

For ‘instantaneous’ (inclusive) broadband operation, commercial UWB antennas are often ‘open’ structures based on monopole antennas (with additional resonant features). These physically protrude from terminals, and show variable pattern performance over the bandwidth concerned. The challenge is, therefore, to design antenna structures that are not excessively large for the terminal application, but flexible in frequency characteristics to facilitate tunable (exclusive) operation over a wide frequency.

Although narrowband, patch antennas may be considered for broadband operation as long as they have sufficient bandwidth for single channel operation and can be tuned over a suitable operating bandwidth. Furthermore, since the resonant frequency is being pulled (rather than other modes being excited), good pattern stability results [12].

#### B. Fixed-frequency Prototype

Here, the cavity-backed linear slot antenna (Figure 1) is proposed as an example of a solution for exclusive mode flexible antenna realization as it can realistically be implemented in a terminal (for instance incorporated into the

casing). The analysis for this type of structure requires consideration of the slot resonances alongside the cavity resonances [13][14]; however, the situation here using a stripline feed (on an electrically-thin substrate) needs only consideration of the cavity as a two-dimensional resonator. The slot’s lowest resonate frequency (for the TE<sub>10</sub> slot mode) is when its length is approximately a half wavelength in air (the dielectric constant of the substrate having a secondary effect on the resonant frequency), while the orthogonal cavity modes’ resonant frequencies depend primarily upon the dimensions and substrate dielectric constant. The input match offered by the stripline feed may be set by its position along the slot and the length of the open stub that extends beyond the slot. The use of the dual-feed arrangement allows different modes to be excited in the structure for pattern diversity and pattern stability over a wide operating range [15]. For instance, with opposite side dual feeds, driving the ports in antiphase will produce a radiation pattern with its maximum in the broadside direction, whilst feeding the elements in-phase will encourage modes in the slot that produce broadside nulls in the pattern [16]. This flexible pattern operation does, however, have implications on input matching for the antenna.

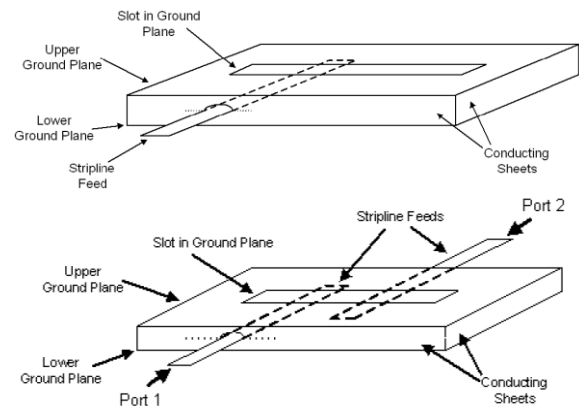


Figure 8. Single- and dual-fed cavity backed slot antennas

Figure 9 shows the measured far-field radiation patterns for an example implementation of a (single feed) cavity backed slot antenna at 2.02GHz. These show the broadside nature of the pattern and the high level of polarization purity.

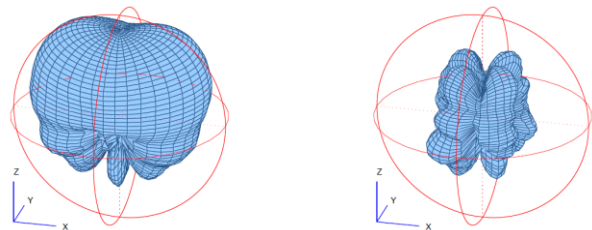


Figure 9. Co-(a) and Cross-polar(b) radiation patterns (relative dB scale with -40dB at centre)

#### C. Frequency Tuning by Length Adjustment

The application of frequency tuning to this controlled-radiation pattern antenna may be via configurable short circuits and/or variable capacitors. Varactor diodes, CMOS switches, optical-gate transistors and PIN diodes are

appropriate enablers should linearity not be an issue. However, if signal (transmitted or received) fidelity is a concern, MEMS technology offers a linear solution [17][18].

The most suitable appliqué of configurable elements to do this is in the form of switches across the slot width in order to form an alternative route for the loop current. In Figure 3, short circuiting wires (to represent ideal switches) have been placed along the slot width. Table 2 gives the design data for an example practical investigation. The results in terms of return loss are given in Figure 4; in which four examples of ‘switch position’ (X) are shown enabling a variation in resonant frequency of over 40%.

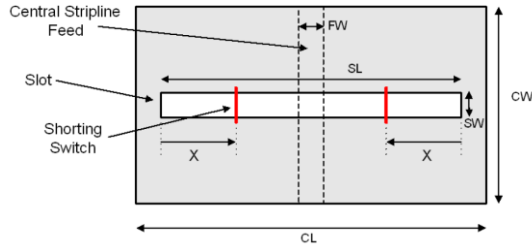


Figure 10. Single-fed length-tuned antenna

TABLE II. DESIGN DATA FOR THE SINGLE-FED LENGTH-TUNED ANTENNA

CL	=	75mm	CW	=	60mm
SL	=	65mm	SW	=	1mm
FW	=	2.7mm	Cavity Height	=	3.2mm
Substrate	=	UltraLam1217	er	=	2.17

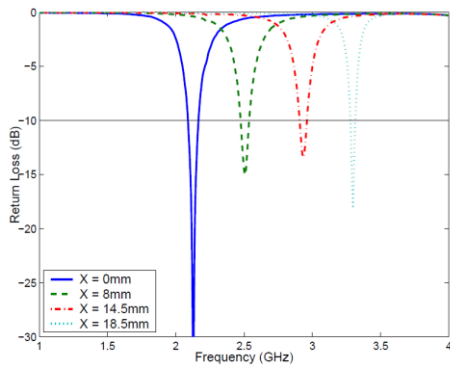


Figure 11. Resonant frequency shifting of the length-tuned antenna

#### D. Frequency Tuning by Susceptance Adjustment

A capacitive configurable element (such a varactor diode) placed across the width of the slot at the centre of its length will also tune the frequency response; however, in contrast to the switching of fixed short circuits, the control is continuous and fine tuning is possible. Whilst not currently commercially available, MEMS topologies exist in the literature for variable capacitances. In the same manner as discrete switches, such devices will maintain linearity in high dynamic range and/or high power applications. The affect of this element is to change the overall input susceptance, and hence the electrical size of the slot. Because of the change in susceptance, it is best to design the geometric shape of the antenna to offer the optimum input match at the centre of the tuning range so that

degradation in input match is balanced (this one degree of freedom will alter both match and resonance, although it can be seen that the match is the most affected). This approach has also been applied to other antenna structures [19].

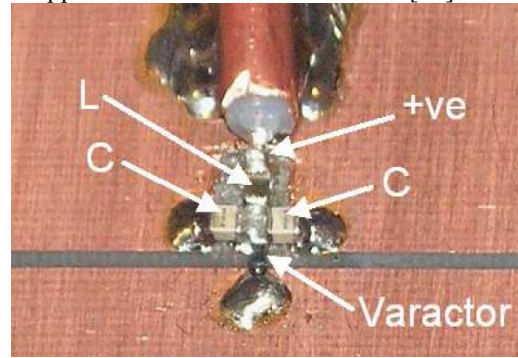


Figure 12. Varactor at the centre of a slot with biasing and RF/DC isolation components shown

A photograph of the appliqué of a Skyworks SMV1763-079 Varactor is given in Figure 12. The result of a modified antenna based on the structure summarized in TABLE II is given in Figure 13.

The maximum resonant frequency is significantly less than that observed in Figure 11 due to the minimum capacitance of the device. However, because this is a bought-in readily available component, the tuning range is faithful to what may be achieved by this method: circa 35%. It should be noted that the drawback with varactor diodes is the affect it has on the overall losses within the structure – where the tuning range is the most (at low voltage bias) the losses are larger; and in the return loss plot, this gives the appearance of increased bandwidth – this is at the expense of antenna efficiency.

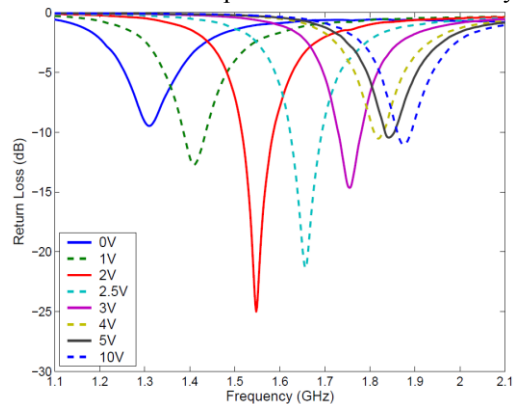


Figure 13. Resonant frequency shifting of the varactor-tuned antenna

In order to demonstrate the validity of applying both tuning methods simultaneously, the experiment was repeated with short circuits at position X=15mm; yielding the result shown in Figure 14. The frequency about which the tuning is centered is higher (as expected) and the percentage tuning range is consistent. However, the combined load mismatch effects of switch and varactor tuning result in appreciable degradation of return loss as the tuned frequency migrates from the centre.

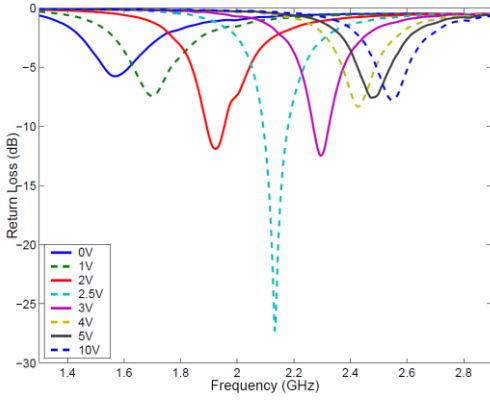


Figure 14. Resonant frequency shifting of the varactor-tuned antenna with short circuits at  $x=15\text{mm}$

The dual feedline antenna may be tuned in the same manner, yet may be controlled to maintain the radiation pattern. The design and design data for an example test antenna built to demonstrate this are given in Figure 15 and TABLE III respectively.

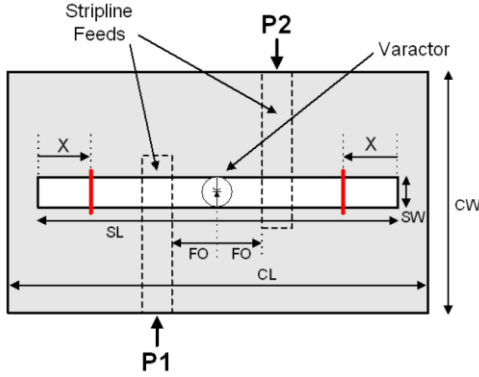


Figure 15. Dual-fed length-tuned antenna

TABLE III. DESIGN DATA FOR THE DUAL-FED LENGTH-TUNED ANTENNA

CL	=	75mm	CW	=	60mm
SL	=	60mm	SW	=	1mm
Feed Length	=	37mm	Feed Width	=	2.7mm
FO	=	5mm	Cavity Height	=	3.2mm
X	=	7mm	$\epsilon_r$	=	2.17
Substrate	=	UltraLam1217			

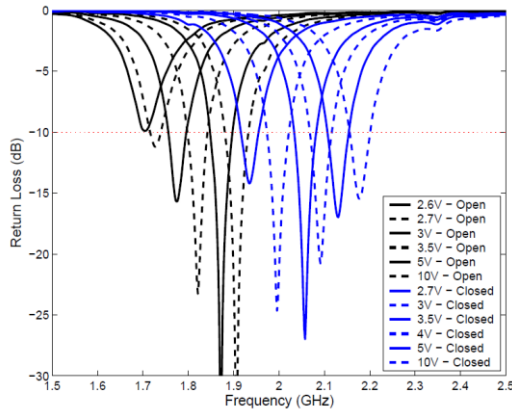


Figure 16. Resonant frequency shifting of the dual-fed varactor- and length-tuned antenna

The return losses for a range of varactor bias voltages with and without shorts at  $x=7\text{mm}$  is shown in Figure 16. The tuning range without shorts is 1.70GHz to 1.93GHz, and with shorts is 1.88GHz to 2.20GHz: an overlap of 50MHz. The combined responses, therefore, exhibit a total operational range of 500MHz, centered at 1.925GHz (chosen to follow current trends in wireless communication standards).

### E. Radiation Patterns

Return loss characteristics, on their own, are a limited measure of the antenna's transmission performance since they offer no indication as to whether the input power is transmitted or dissipated. The radiation pattern of the dual feedline antenna was measured in 3-dimensions using a certified anechoic chamber. A consistent pattern with good characteristics over the entire operational bandwidth is the design aim for an antenna for handset applications.

The co- and cross-polar radiation patterns for the antenna at 2.178GHz are shown in Figure 17: The pattern, measured with shorts and a varactor bias voltage of 10V, shows the desired TE<sub>10</sub> slot mode. The perturbation to the rectangular slot, necessary for the incorporation of the varactor's bias circuitry, therefore, had no observable effect on the antennas radiation pattern or polarization. Visual comparison of Figure 17 and Figure 9 gives the subjective result that the pattern is essentially unaffected by the appliques of shorts and varactor.

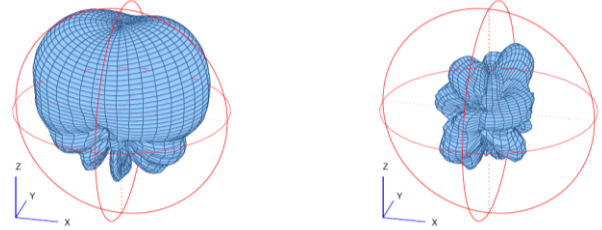


Figure 17. Co-(a) and Cross-polar(b) radiation patterns (relative dB scale with -40dB at centre)

The radiation patterns were measured with varied varactor bias voltages, both with and without the shorts. The patterns were correlated with that at 2.178GHz (Figure 17) and the radiation pattern statistics are given in TABLE IV. The changes in co-polar radiation at the limits of voltage bias and short states are shown in Figure 18. It is worth noting that the radiation pattern is essentially consistent over the separate resonant frequencies.

TABLE IV. VARIATION STATISTICS FOR THE RADIATION PATTERN ACROSS CONFIGURED STATES

Frequency (Ghz)	Bias (V)	Short/Open	Correlation Coef (%)	Co-polar Power (%)	Directivity (dBi)
1.728	2.7	O	91	88	6.3
1.821	3.5	O	92	90	6.1
1.96	10	O	27	94	6.8
1.936	2.7	S	95	85	7.2
2.056	3.5	S	99	96	7.5
2.178	10	S	100	96	7.5

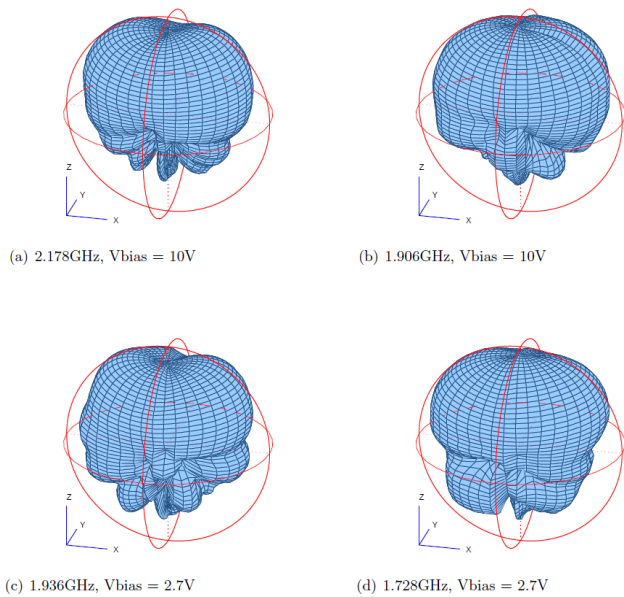


Figure 18. Co-polar radiation patterns (relative dB scale with -40dB at centre) for example tuned points of operation

The general radiation pattern performance was consistent with the same mode dominant over the entire bandwidth. The variation in radiation pattern was negligible compared to the extreme change that would have resulted from other modes becoming dominant. It should be noted that the consistency of the radiation pattern did not arise from ad-hoc control of the dual feed excitation phase relationship; it is the presence of the dual feeds that suppresses the excitation of other modes as operating frequency changes.

#### IV. CONCLUSION

This paper introduced solutions for the delivery of a flexible microwave filters and antennas for SDR and CR. The former is based on lumped-distributed coupled lines and the latter is based on the cavity-backed linear slot approach. The structures are designed to be ready for MEMS actuation, a technology which is proposed here as being highly appropriate for product realization.

For the filter both  $F_c$  and B/W tuning is realized and results of both simulation and practical measurements show good flexibility in the spectral performance. For the Antenna, two tuning methods are presented with results of practical measurements of both return loss and radiation pattern. Good consistency is shown in the radiation pattern as the centre frequency of the antenna is tuned by variations of input susceptance and effective length.

#### V. ACKNOWLEDGEMENTS:

The authors acknowledge the following (past) PhD students at The University of Bristol. Although not direct contributors to

this paper, supporting documentation and research results were gratefully received.

Dr Henry Hunt-Grubbe

Dr Bruce Carey-Smith

- [1] MITOLA J. III, 'The software radio architecture', IEEE Communications Magazine, May 1995, vol. 33 of 5, pp. 26-38
- [2] MAGUIRE G.Q. MITOLA J. III, 'Cognitive radio: Making radio more personal', IEEE Personal Communications Magazine, August 1999
- [3] JONDRAL F.K., 'Software-defined radio - basics and evolution to cognitive radio', Journal on Wireless Communications and Networking. EURASIP, 2005, 3, pp. 275-233
- [4] B. E. CAREY-SMITH, P. A. WARR, P. R. ROGERS, M. A. BEACH, AND G. S. HILTON, "Flexible frequency discrimination subsystems for reconfigurable radio front ends," EURASIP Journal on Wireless Communications and Networking, vol. 2005, no. 3, 2005.
- [5] D. CABRIC, S. M. MISHRA, AND R. W. BRODERSEN, "Implementation issues in spectrum sensing for cognitive radios," in Conference Record of the Thirty-Eighth Asilomar Conference on Signals, Systems and Computers., vol. 1, Nov. 2004, pp. 772-777.
- [6] ARMSTRONG E.H., 'The superheterodyne: Its origin, development, and recent improvements', Proc. I.R.E., October 1924, pp. 539-552
- [7] GU Q., 'RF System Design of Transceivers for Wireless Communications - Chapter 3.2, Springer, 2005, ISBN: 9780387241616
- [8] ROGERS P. BEACH M.A. HILTON G.S. CAREY-SMITH B., WARR P.A., 'Flexible frequency discrimination subsystems for reconfigurable radio front ends,' Wireless Communications and Networking, EURASIP, March 2005, pp. 354-363
- [9] J-S. HONG, M. J. LANCASTER, "Couplings of microstrip square open-loop resonators for cross-coupled planar microwave filters," IEEE Trans. Microwave Theory Tech., vol. MTT-44, pp. 2099 -2109, Nov. 1996.
- [10] CAREY-SMITH, B.E.; WARR, P.A.; BEACH, M.A.; NESIMOGLU, T., 'Wide Tuning-Range Planar Filters Using Lumped-Distributed Coupled Resonators', IEEE Transactions on Microwave Theory and Techniques, Volume: 53, Issue: 2, Feb. 2005, pp. 777 - 785.
- [11] BAHL I.J. ITTIPIBOON A. GARG R., BHARTIA P., 'Microstrip Antenna Design Handbook', Chapter 7, Artech House, 2001, ISBN: 0890065136
- [12] RAILTON C.J. ROSTBAKKEN O., HILTON G.S., 'Adaptive feedback frequency retuning of microstrip patch antennas,' 9th International Conference on Antennas and Propagation. IEEE, April 1995, vol. 1.
- [13] HAMID M. HADIDI A., 'Aperture field and circuit parameters of cavity-backed slot radiator', IEE Proceedings, April 1989, vol. 136 of 2
- [14] GALEJS J., 'Admittance of a rectangular slot which is backed by a rectangular cavity,' IEEE Transactions on Antennas and Propagation, March 1963, vol. AP-11, pp. 119-126
- [15] HILTON G.S. HUNT-GRUBBE H.W.W., 'Radiation pattern performances of single feed and differentially driven dual feed cavity backed linear slot antennas,' Loughborough Antennas and Propagation Conference, Loughborough, UK, April 2006, IEE
- [16] HILTON G.S., URWIN-WRIGHT P., HUNT-GRUBBE H.W.W., 'The analysis of balanced feed antenna structures for use in integrated antenna-transceivers', IEE, 2003, ICAP, University of Exeter, UK
- [17] REBEIZ G.M., 'RF MEMS. Theory, design and technology', Wiley, 2003, ISBN: 0-471-20169-3
- [18] JOSE K.A. VARADAN V.K., VINOY K.J., 'RF MEMS and their applications', Wiley, 2003, ISBN: 0-470-84308-X
- [19] CRADDOCK I.J. FLETCHER P.N. URWIN-WRIGHT P.R., HILTON G.S., 'A tunable electrically-small antenna operating in the dc mode,' in 5th European Personal Mobile Communications Conference, Glasgow, 2003, IEE